Food Hydrocolloids 25 (2011) 1051–1062

Contents lists available at ScienceDirect

Food Hydrocolloids

journal homepage: www.elsevier.com/locate/foodhyd

Hydroxypropylmethylcellulose at the oil–water interface. Part II. Submicron-emulsions as affected by pH

Nerina A. Camino, Ana M.R. Pilosof*

CONICET, Departamento de Industrias, Facultad de Ciencias Exactas y Naturales, Ciudad Universitaria, Universidad de Buenos Aires, Intendente Guiraldes 2160, C1428EGA, Buenos Aires, Argentina

ARTICLE INFO

Article history:
Received 13 July 2010
Accepted 30 September 2010

Keywords:
Hydroxypropylmethylcellulose
High intensity ultrasound
Emulsions
Stability
Interface

ABSTRACT

The emulsifying behavior of four different commercial types of hydroxypropylmethylcellulose (HPMC) was studied and correlated with the properties of the interfacial films.

Emulsions resulted multimodal when made by a high speed blender (Ultraturrax, UT), with droplets higher than 10 μm. The average diameters D_{32} resulted higher for UT emulsions stabilized by the higher molecular weight HPMC (E4M and E50LV). However, E4M emulsions presented the highest variation in D_{32} with pH.

Emulsions made by high intensity ultrasound, presented a monomodal population with the majority of the droplets around 0.3 μm. In all cases, the droplets sizes were smaller than 0.5 μm. As for UT emulsions, higher average diameters (D_{32} and D_{43}) were obtained for all HPMCs at pH3.

Emulsions at pH3 destabilized quicker than emulsions at pH6, mainly when made by Ultraturrax. At pH3 hydrophobic interactions are impeded thus elastic films are not formed upon emulsification, resulting in droplets with higher initial diameters than at pH6.

1. Introduction

Emulsions are thermodynamically unstable systems and tend to separate in order to minimize the interfacial area between the aqueous and the oil phase, yet they are among the most important colloids in numerous applications in the food and pharmaceutical industry. Long term physical stability is crucial, and kinetic stability is clearly an important goal in the development of a new emulsion formulation. Common requirements of a stable emulsion over the time scale of desired shell-life are no discernible changes in size distribution of the droplets or their state of aggregation, or in the spatial arrangement within the vessel (Dickinson, 2003). This can only be achieved by adequate control of the instability processes which often is challenging since emulsion instability is a complex process and may involve a combination of different mechanisms such as creaming or sedimentation, flocculation and coalescence (Friberg & Larsson, 1997; Sjöblom, 1996).

Typically, the droplet size of conventional emulsions is larger than 1 μm, making these droplets susceptible to gravity forces. Depending on the preparation method, different droplet size distributions might be achieved, explaining why the route of preparation can have an influence on the emulsion stability (Fernandez, André, Rieger, & Kühnle, 2004). The formation of an emulsion may involve a single step or a number of consecutive steps, depending on the nature of the starting material and the method used to create it (McClements, 1999).

Nano-emulsions are a class of emulsions with a droplet size between 20 and 500 nm (Fernandez et al., 2004; Porras et al., 2004; Weiss, Takhistov, & McClements, 2006). Due to their characteristic size, nano-emulsions possess high stability against sedimentation or creaming (Solans, Izquierdo, Nolla, Azemar, & Garcia-Celma, 2005).

The preparation of emulsions with droplet sizes in the sub-micrometer range involves high – energy input that is generally achieved by high–shear stirring, high-pressure homogenizers or by ultrasound generators (Weiss et al., 2006).

Schulz and Danields (2000) have reported the obtention of submicron-emulsions with shorter chained HPMC using a high-pressure homogenizer. Gu, Decker, and McClements (2005) also obtained multilayer nano-emulsions stabilized with β-lactoglobulin, ι-carrageenan and gelatin using also a high-pressure homogenizer. Alvarez Cerimedo, Huck Iriart, Candal, and Herrera (2010) reported submicron-emulsions stabilized by sodium-caseinate and trehalose homogenizing with an high intensity ultrasound equipment.

Another important factors influencing the functionality of an emulsion are the interfacial properties of the emulsifier used. An

* Corresponding author. Tel.: +54 11 4576 3377; fax: +54 11 4576 3366.
E-mail address: apilosof@di.fcen.uba.ar (A.M.R. Pilosof).

0268-005X/$ – see front matter © 2010 Elsevier Ltd. All rights reserved.
doi:10.1016/j.foodhyd.2010.09.026

effective emulsifier should rapidly adsorb to the freshly formed droplet surface, reduce the interfacial tension by an appreciable amount to facilitate droplet disruption and provide a protective coating that prevents the droplets from aggregating with their neighbors (McClements, 2004).

There are two classes of molecules that have a strong tendency to adsorb at fluid interfaces: proteins and small molecule surfactants (Courthaudon & Dickinson, 1991). Most high molecular weight polysaccharides, being hydrophilic, do not have much tendency to adsorb at the air water interface. However, some gums have been found to stabilize emulsions and exhibit interfacial activity (Baeza, Carrera Sanchez, Pilosof, & Rodríguez Patino, 2004; Huang, Kakuda, & Cui, 2001; Perez, Carrera Sanchez, Rodriguez Patino, & Pilosof, 2006). The hydroxypropylmethylcelluloses are included in this group.

The resulting ability of HPMCs to reduce the interfacial tension as well as increase the viscosity of the water phase make them suitable as emulsifying agents. Some studies have been reported on the use of HPMC in oil-in-water emulsions (Daniels & Barta, 1993, 1994; Kiekens, Vermeire, Samyn, Demeester, & Remon, 1997; Schulz & Danields, 2000; Wollenweber, Makievski, Miller, & Daniels, 2000). Additionally, the usefulness of HPMC for the food or pharmaceutical industry is based upon its capacity to form reversible thermal gels that melt upon cooling (Perez, Wargon, & Pilosof, 2006; Yuguchi, Urakawa, Kitamura, Ohno, & Kajiwara, 1995).

This work is part of a more comprehensive study, which leads to a consistent understanding of the main properties of HPMC at interfaces, foams and emulsions. In previous works we determined the dynamic and equilibrium characteristics of the HPMCs at the sunflower oil–water interface (Camino, Carrera Sanchez, Rodriguez Patino, & Pilosof, 2011; Camino, Perez, Carrera Sanchez, Rodriguez Patino, & Pilosof, 2009). We found that the dynamic light scattering analysis of particle size distribution in HPMC water solutions indicated cluster formation at pH6 for most types. The dynamics of adsorption showed that the surface pressure (π) values and the rate of adsorption/penetration were lower at pH3. The surface dilatational modulus of films at pH6 showed a continuous increase indicating a slow formation of a viscoelastic interfacial film. Nevertheless, at pH3 in most cases a viscoelastic film was not formed.

Among all the HPMC studied, E5LV showed over all the best performance at this oil–water interface due to its low molecular weight and high decrease of interfacial tension. Its high hydrophobicity allows a strong tendency to interact at the interface and form elastic films.

Thus, the aim of the present work was study the performance of the same four different types of HPMC in emulsions at pH3 and pH6 and the impact of interfacial properties on emulsions characteristics.

2. Materials and methods

2.1. Materials

Methocell E5LV, E15LV, E50LV and E4M (food grade) from the Dow Chemical Company were kindly supplied by Colorcon Argentina and used without purification. Table 1 shows some characteristic properties, such as methyl and hydroxypropyl content, methyl/hydroxypropyl ratio, molar substitution, the degree of substitution, the viscosity (20 °C) of 2%wt solutions, and molecular weight. The moisture content of HPMC powders was 1.6%.

HPMC solutions at 2%wt, were prepared at 90 °C by dispersing the powder in buffer Sörensen solutions, phosphate for pH6 or citrate/chlorine for pH3, and cooled down to room temperature. Milli–Q ultrapure water was used for buffer preparation. The pH and ionic strength ($I = 5$ mM) were kept constant. The solutions were stored at 4 °C for 24 h to achieve the maximum polysaccharide hydration.

Table 1
Properties of E4M, E50LV, E15LV and E5LV.

HPMC	E4M	E50LV	E15LV	E5LV
% methyl	28.0	29.1	29.2	29.5
% hydroxypropyl	10.2	9.2	9.3	9.7
Methyl/hydroxypropyl ratio	2.3	3.2	3.1	3.0
Methyl substitution (DS)	1.90	1.90	1.90	1.90
Hydroxypropyl substitution (MS)	0.23	0.23	0.23	0.23
Total substitution (DS + MS)	2.13	2.13	2.13	2.13
Viscosity (cp), 2% wt solution, 20 °C	4965	41	15	5.4
Molecular weight (Da)	90000	18000	6000	2000

Commercial sunflower oil was used as the oil phase in this research without further purification in order to study the performance of HPMCs in a real interface (i.e. commercial oil widely used in the food industry).

2.2. Methods

2.2.1. Emulsion preparation

2.2.1.1. Ultraturrax (UT). The oil and HPMC solutions were emulsified in a 10:90 ratio respectively, for 3.5 min at room temperature, using a high speed blender, Ultraturrax T8 (IKA – WERKE, GMBH & Co. KG, Staufen, Germany) at 25000 RPM, with a dispersion unit S8 N-5G.

2.2.1.2. High-intensity ultrasound (HIUS). The oil and HPMC solutions were emulsified in a 10:90 ratio, for 20 min, using an ultrasonic processor Vibra Cell Sonics, model VCX 750 (Sonics & Materials Inc., Newtown, CT, United State) at a frequency of 20 kHz and an amplitude of 20%. A 13 mm (1/2 inch) high grade titanium alloy probe threaded to a 3 mm tapered microtip was used to sonicate 5 ml of sample in a 15 ml glass tube reactor that was glycerine – jacketed at 0 °C with a circulating constant temperature cooling bath (Polystat, Cole–Parmer). At this temperature, the heat produced during sonication was dissipated, keeping the sample temperature below 25 °C.

In some experiments, premixing of oil and HPMC solutions was done with the UT at 25000 RPM for 1 min at room temperature and further homogenized for 20 min with HIUS.

2.2.2. Droplet size distribution

The droplet size of emulsions was measured by light scattering using a Mastersizer 2000 with a Hydro 2000MU as dispersion unit (Malvern Instruments, Worcestershire, United Kingdom). The pump speed was setted at 1800 RPM. The refractive index (RI) of the disperse phase (1.47) and its absorption parameter (0.001) was used. The RI of the interfacial HPMC layer was not taken into account because when considered, the change produced was less than 1%, taking into account that the thickness of an adsorbed layer is about 2–10 nm (McClements, 1999). Droplet size is reported as the volume-surface mean diameter or Sauter diameter ($D_{32} = \Sigma n_i d_i^3/\Sigma n_i d_i^2$) and the equivalent volume-mean diameter or De Broucker diameter ($D_{43} = \Sigma n_i d_i^4/\Sigma n_i d_i^3$), where n_i is the number of droplets of diameter d_i (Galazka, Dickinson, & Ledward, 1996; Gu et al., 2005; Guzey, Kim, & McClements, 2004; Huang et al., 2001; Leroux, Langendorff, Schick, Vaishnav, & Mazoyer, 2003).

D_{32} provides a measure of the mean diameter where most of the particles fall (Gu et al., 2005). D_{43} is related with changes in particle size involving destabilization processes so is more sensitive to fat droplet aggregation (Alvarez Cerimedo et al., 2010; Relkin & Sourdet, 2005).

The specific surface area (SSA) and the polidispersity obtained by the software are also reported.

The polidispersity is calculated as: $(D_{0.9} - D_{0.1})/D_{0.5}$ where 10, 50 and 90% represent the oil volume in the emulsion contained in droplets with diameters below or equal to $D_{0.1}$, $D_{0.5}$ and $D_{0.9}$ respectively. The SSA is calculated using the diameter D_{32} (Carrera Sanchez & Rodriguez Patino, 2005; Cornec et al., 1998).

The droplet sizes are reported as the average and standard deviation of ten readings made on a sample.

2.2.3. Zeta potential measurements

Zeta potential measurements (ξ) were carried out in a Dynamic Laser Light Scattering instrument (Zetasizer Nano-Zs, Malvern Instruments, Worcestershire, United Kingdom) provided with a He–Ne laser (633 nm) and a digital correlator, Model ZEN3600. Measurements were carried out at a fixed scattering angle of 17°. Emulsions at 2% wt were previously diluted 1:100 to a droplet concentration of 0.02% wt with the corresponding buffer solution and then contained in a measurements chamber of a particle electrophoresis instrument. The zeta potential was determined by measuring the direction and velocity of the droplets moving in the applied electric field at 25 °C. The zeta potential measurements are reported as the average and standard deviation of measurements made on two samples, with ten readings made per sample.

The Zetasizer Nano series calculates the zeta potential by determining the Electrophoretic Mobility and then applying the Henry equation. The electrophoretic mobility is obtained by performing an electrophoresis experiment on the sample and measuring the velocity of the particles using Laser Doppler Velocimetry (LDV).

Henry equation:

$$U_E = \frac{2\varepsilon z f(\mathrm{ka})}{3\mu} \quad (1)$$

where, z is the Zeta potential, U_E is the Electrophoretic mobility, ε is the Dielectric constant, μ is the Viscosity, and f(Ka) is the Henry's function. Two values are generally used as approximations for the f (Ka) determination either 1.5 or 1.0. In aqueous media and low electrolyte concentration, as in this work, the 1.0 value is used (Huckel approximation).

2.2.4. Emulsion viscosity

The emulsion viscosity was determined in a Brookfield DV-LVT viscometer (Brookfield Engineering Laboratories, Inc., Middleboro, United States) with a cone-plate arrangement at 25 °C without previous dilution. The cones CP41 and CP52 of diameter 4.8 mm and 2.4 mm respectively were used. The deformation velocities were setted in the range of 0.5 and 120 s^{-1}.

The shear stress vs. deformation velocities curves were obtained. The results were adjusted using the power law:

$$\tau = K \cdot \upsilon^n \quad (2)$$

where τ is the shear stress, υ is the deformation velocity, K is the consistent index, n is the flux index.

The viscosity measurements are reported as the average and standard deviation of at least three samples.

2.2.5. Emulsion stability

The global stability of emulsions was determined through the use of a vertical scan analyzer Turbiscan MA 2000 (Formulaction, Toulouse, France). This equipment allows the optical characterization of any type of dispersion (Alvarez Cerimedo et al., 2010; Mengual, Meunier, Cayré, Puech, & Snabre, 1999). The reading head is composed of a pulsed near-IR light source ($\lambda = 850$ nm) and two synchronous detectors. The transmission detector receives the light, which goes through the sample (0°), while the backscattering detector receives the light back scattered by the sample (135°) (Alvarez Cerimedo et al., 2010).

The samples were put in a flat-bottomed cylindrical glass measurement cell and scanned from the bottom to the top in order to monitor the optical properties of the dispersion along the height of the sample placed in the cell. The backscattering (BS) and transmission (T) profiles as a function of the sample height (total height = 60 mm) were studied in quiescent conditions at 25 °C. In this way, the physical evolution of this process is followed without disturbing the original system and with good accuracy and reproducibility (Alvarez Cerimedo et al., 2010; Mengual et al., 1999). Thus, by repeating the scan of a sample at different time intervals, the stability or the instability of dispersions can be studied in detail. The profiles allow calculation of either creaming, sedimentation or phase separation rates, as well as flocculation and the mechanism making the dispersion unstable can be deduced from the transmission or the backscattering data (Alvarez Cerimedo et al., 2010). The emulsions recently prepared were loaded into the measurement cell and the backscattering percentage profiles (%BS) all along the tube were immediately monitored every 5 min for emulsions prepared with UT and every 15 min for emulsions prepared with USAI during the first 2 h. The cells were stored at room temperature for 20 days and another individual value for %BS was taken every 24 h.

The curves obtained by subtracting the BS profiles at $t = 0$ from the profile at $t = t$ ($\Delta BS = BS - BS0$), display a typical shape that allows a better quantification of creaming, flocculation and other destabilization processes.

Creaming was detected using the Turbiscan as it induced a variation of the droplets concentration between the top and the bottom of the cell. The droplets moved upward because they had a lower density than the surrounding liquid. When creaming takes place in an emulsion, the ΔBS curves show a peak at heights between 0 and 20 mm. The variation of the peak wide, at a fixed height, during the studied time, can be related to the kinetics of migration of small particles (Alvarez Cerimedo et al., 2010; Mengual et al., 1999). The creaming destabilization kinetics was evaluated by measuring the peak width at 50% of the height at different times (bottom zone). The slope of the linear part of a plot of peak width vs. time gives an indicator of the migration rate (Alvarez Cerimedo et al., 2010).

BS mean values (BSav) change with the increasing particle size. Flocculation was followed by measuring the BSav as a function of storage time in the middle zone of the tube. The optimum zone was the one not affected by creaming (bottom and top of tube) that is, the 20–50 mm zone.

The results are reported as the average and standard deviation of at least two samples.

2.2.6. Microstructure

The Olympus FV300 (Olympus Ltd., London, UK) confocal laser scanning microscope (CLSM) with a Ar gas laser ($\lambda = 488$ nm) was used to collect the images. A 2.5× ocular was used, together with a 60× objective for a visual magnification of 150×. The laser intensity used was 20%. Images were recorded by using confocal assistant Olympus Floview version 3.3 software provided with the FV300 CLSM.

2.2.7. Statistical analysis

The data was statistically analyzed with the program Statgraphic 5.1 plus. All the measurements were conducted and reported as means ± 95% confidence limits. Statistical analysis was performed using t-test and one-way analysis of variance (ANOVA) to identify

which groups were significantly different from other groups ($P < 0.05$).

3. Results and discussion

3.1. HPMC emulsion droplet size distribution

3.1.1. Droplet size distribution of emulsions homogenized with Ultraturrax (UT)

Fig. 1 shows the droplet size distribution for 10/90 O/W emulsions respectively, prepared with UT at pH3 and 6 (Fig. 1A and B respectively). At both pHs, the droplet size distributions were trimodal for all the HPMCs, with a predominance of population II (peak maximum at 10 μm). Mitidieri and Wagner (2002) and Palazolo (2006) also obtained trimodal distributions when studying soy protein stabilized emulsions prepared with UT.

Population I has the maximum peak at 0.2 μm for all the HPMCs emulsions at pH6 (Fig. 1B) and for E5LV and E15LV at pH3 (Fig. 1A). This peak shifted to 0.3 μm for E50LV emulsions and to 1 μm for E4M emulsions at pH3.

Population III presents a maximum at 100 μm for both pHs. E5LV, E15LV and E50LV emulsions at pH3 presented a small proportion of these droplets size but was predominant for E4M emulsions. Only E5LV emulsions did not present droplets at this size range at pH6 (Fig. 1B).

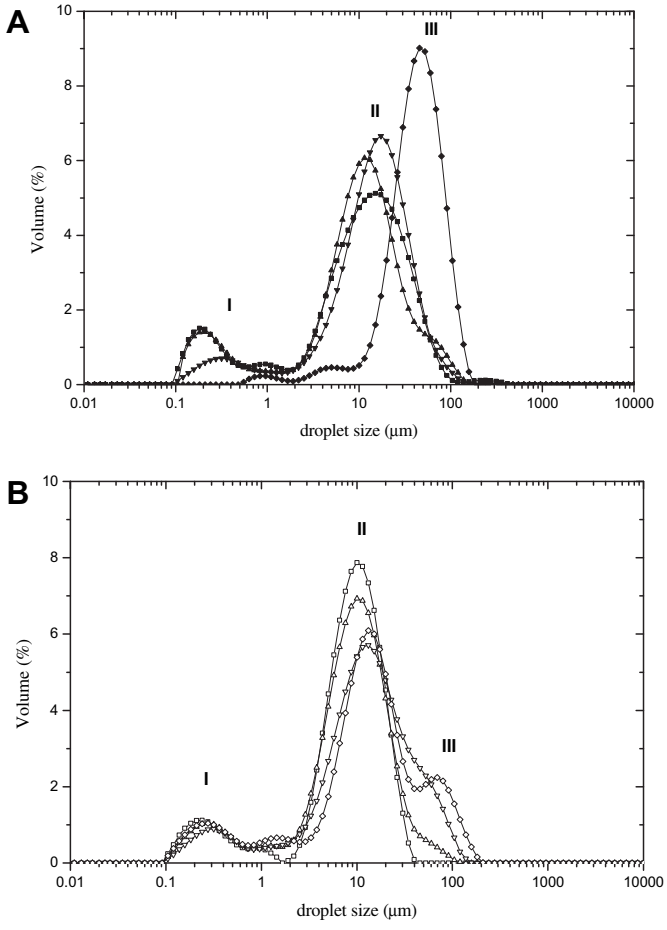

Fig. 1. Volume droplet size distribution (%) of 2% wt O/W HPMC emulsions homogenized with Ultraturrax at pH3 (A) and pH6 (B). E5LV (■,□), E15LV (▲,△), E50LV (▼,▽) and E4M (◆,◇). I: droplets in population I, II: droplets in population II and III: droplets in population III.

The number droplet size distributions (not shown) were similar for all the HPMCs emulsions and presented a high proportion of droplets in the range of population I and less in the range of population II. This means that population I contributed largely to the area created during the homogenization process but did not contribute to the total volume of the dispersed phase (Palazolo, 2006). Population II and III concentrated almost all the volume of the dispersed phase of the emulsions. Ventureira, Martinez, and Añon (2010) studying amaranth proteins emulsions, also found that the population lower than 2 μm did not contribute to the total volume of the dispersed phase but its importance increased if the area created during the homogenization process is considered.

The behavior of these colloidal systems, when referring to creaming and coalescence, is governed by the presence of higher droplet sizes, even when they represent a small proportion of the total number of droplets in the emulsion (McClements, 1999). When higher are the droplet sizes in an emulsion, it would present a higher tendency to coalescence induced by collision. The impact forces and their magnitude during a collision are higher when higher is the droplet size (McClements, 1999).

Table 2 shows the average diameters, the polidispersity and the specific surface area for the HPMCs emulsions recently prepared with UT.

During the homogenization process with a high velocity agitator (UT), the aqueous and oily phases are submitted to an intense mechanical agitation in laminar and turbulent regime. In consequence, the resulting interfacial area is a balance between the rupture (interfacial area creation) and coalescence (interfacial area reduction) processes (McClements, 1999; Palazolo, 2006; Walstra, 1993).

In this work, the homogenization conditions were equal for all the emulsions, so the SSA variation is mainly attributed to the HPMCs used, which favored or inhibited the processes before mentioned. When lowest the D_{32}, higher the SSA.

The average diameter D_{32} decreased with the molecular weight of HPMCs (Tables 1 and 2). Nevertheless at pH3 E4M exhibited a much higher D_{32} value than the other HPMCs.

Hayakawa, Kawaguchi, and Kato (1997) also found that the size of the oil droplet of HPMC-silicone oil emulsions increased with the molecular weight of HPMC at a fixed concentration of the polysaccharide.

The polidispersity and the D_{43} diameters, related with the destabilization processes, were higher for all the emulsions at pH3.

In a recent work (Camino et al., 2011) we reported that the interfacial films of HPMCs at pH3 presented a low viscoelasticity and poor solid character. The interfacial film around the oil droplets should be strong enough to avoid the fusion of them during the homogenization process (McClements, 1999; Palazolo, 2006). In consequence, pH3 emulsions would present a higher tendency to coalescence during their formation.

Sun, Sun, Wei, Liu, and Zhang (2007) also demonstrated that the hydrophobically modified hydroxyethylcellulose (HMHEC) could form a solid film at the oil–water interface and prevent the coalescence of the emulsion droplets.

Table 2
Average diameters de Sauter (D_{32}), De Brouker (D_{43}), polidispersity and specific surface area (SSA) from 2% wt HPMCs emulsions prepared with UT. Maximum standard deviation: 5%.

HPMC	E4M		E50LV		E15LV		E5LV	
	pH3	pH6	pH3	pH6	pH3	pH6	pH3	pH6
D_{32} (μm)	21.30	2.92	2.91	2.48	1.51	1.99	1.44	1.81
D_{43}(μm)	52.21	25.41	20.31	20.91	17.24	12.77	18.74	10.77
polidispersity	4.95	3.89	4.53	3.76	3.43	2.54	4.16	2.16
SSA	0.28	2.98	2.07	2.42	3.00	3.98	3.14	3.32

Dickinson (2001) studied the influence of the interfacial properties in whey protein stabilized emulsions and found that surface interfacial rheology had a great influence in the emulsion stability. Carrera Sanchez and Rodriguez Patino (2005) also observed a correlation between the stability of sodium-caseinate emulsions and the equilibrium surface pressure, the dilatational modulus and the surface viscosity.

The polidispersity followed the same order as the HPMCs molecular weight (Table 2, E4M > E50LV > E15LV > E5LV). This order was also evident in the droplet size distributions (Fig. 1), mainly in population II.

The lower molecular weight HPMCs (E15LV and E5LV) resulted more efficient as their emulsions showed the lower droplets sizes (D_{32} and D_{43}) at both pHs. As discussed previously (Camino et al., 2011) these HPMCs could produce a faster increase in the interfacial pressure and could generate elastic interfacial films.

The viscosity of the continuous phase has also influence in the formed droplet size. Huang et al. (2001) sustained that the viscosities of gums dispersions may have contributed to the observed differences in emulsion stability. The viscosity is a qualitative measurement of the molecular interactions, the higher the viscosity the higher the attractive forces between the polysaccharide molecules and the higher the energy delivered to the system to obtain smaller droplet sizes (Behrend, Ax, & Schubert, 2000). The emulsion viscosity is influenced by various factors, mainly by the continuous phase viscosity, interfacial film viscosity and droplet size. For all the HPMCs emulsions analyzed (Table 3), the consistent index followed the same order of molecular weight/viscosity (Table 1), being E4M emulsions the most viscous.

3.1.2. Droplet size distribution of emulsions homogenized with high intensity ultrasound (HIUS)

There are in the literature several works where a pre-emulsion is prepared previously to the ultrasound or high-pressures treatments (Alvarez Cerimedo et al., 2010; Carrera Sanchez & Rodriguez Patino, 2005; Gu et al., 2005; Schulz & Danields, 2000) to obtain smaller droplet size.

In consequence, it was determined if premixing the HPMCs solutions and oil with UT for 1 min and then treated with HIUS for 20 min would deliver to smaller sizes (Fig. 2). It can be observed, as example for E5LV 2%, that the HIUS emulsion was monomodal with the peak maximum at 1 μm. The pre-mixed emulsion before the HIUS treatment resulted multimodal with well defined four populations. There are two populations with droplet size higher than 10 μm, one with a peak maximum at 30 μm and the other one at 200 μm. The major population presented a peak maximum at 2 μm. Behrend et al. (2000) suggested that a wide range of ultrasound frequencies is necessary to obtain a predominant droplet size in an emulsion and thus a monomodal and narrow distribution. McClements (1999) pointed out that ultrasound homogenizers are capable of producing emulsions with small droplet sizes directly from separate oil and water phase. Therefore, in the present work the HPMCs solutions and oil phase were directly homogenized with HIUS.

Table 3
Flow parameters of HPMC 2%wt emulsions prepared with UT, obtained by Ostwald model.

HPMC	pH3		pH6	
	K	*n*	*K*	*n*
E5LV	0.050 ± 0.006	1.036 ± 0.025	0.340 ± 0.087	0.927 ± 0.055
E15LV	0.272 ± 0.067	1.015 ± 0.077	0.377 ± 0.005	0.917 ± 0.006
E50LV	0.273 ± 0.063	1.015 ± 0.073	5.399 ± 0.304	0.935 ± 0.012
E4M	43.030 ± 1.056	1.034 ± 0.026	67.370 ± 1.833	1.024 ± 0.047

K: consistence flow index (N $m^{-2}s^{-n}$).
n: flow index.
$R^2 > 0.97$.

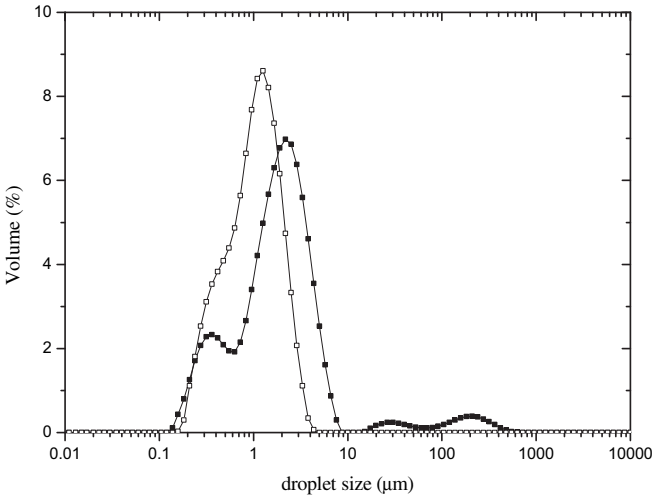

Fig. 2. Volume droplet size distribution (%) of 2% wt O/W pH6 E5LV emulsions homogenized with high intensity ultrasound for 20 min (◇) and pre-emulsified with Ultraturrax during 1 min (◆).

Fig. 3 shows the droplet size distribution for 10/90 O/W emulsions, prepared with HIUS. The populations were almost bimodal at both pHs. E5LV, E15LV and E50LV emulsions resulted polidispersed with a broad population between 0.15 μm and 3 μm and the peak maximum at 1 μm E4M emulsions presented droplets between 0.15 μm and 6 μm with the peak maximum of the principal population at 2 μm.

The number droplet size distributions (not shown) were similar for all the HPMCs emulsions and presented a monomodal population with the majority of the droplets around 0.3 μm. In all cases, the droplets size was smaller than 0.5 μm. This means that the droplets with sizes higher than 0.5 μm contribute largely to the total volume of the dispersed phase but not to the area created during the homogenization process with HIUS.

It is important to point out that all the droplet sizes for HIUS emulsions were below 2 μm. This implicates a higher stability since higher droplet sizes accelerate the destabilization processes as creaming and flocculation (McClements, 1999). The HIUS emulsions should have higher stability than UT emulsions since the last ones present droplet sizes higher than 10 μm and trimodal distributions in almost all cases (Fig. 1).

Table 4 shows the average diameters, the polidispersity and the specific surface area for emulsions recently prepared with HIUS. When comparing the UT emulsions (Table 2 and Fig. 1) and the HIUS emulsions (Table 4 and Fig. 3), it can be observed a high influence of the homogenizer used. The emulsions prepared with HIUS presented lower average diameters and polidispersity for all the HPMCs studied. The specific surface area (SSA) created was remarkable higher for HIUS emulsions which is associated with lower droplet size (Carrera Sanchez & Rodriguez Patino, 2005).

As for UT emulsions, higher average diameters (D_{32} and D_{43}) are obtained for all HPMCs at pH3 for HIUS emulsions (Table 4). The polidispersity also followed the same order of decreasing HPMC molecular weight (E4M > E50LV > E15LV > E5LV). The E4M resulted more polidispersed at both pHs, which is reflected in the distribution curve (Fig. 4). The SSA was higher for all HIUS emulsions at pH6 and the lower molecular weight HPMCs also resulted more efficient to obtain lower droplet sizes (D_{32} and D_{43}) at both pHs. Schulz and Danields (2000) when studying HPMC O/W

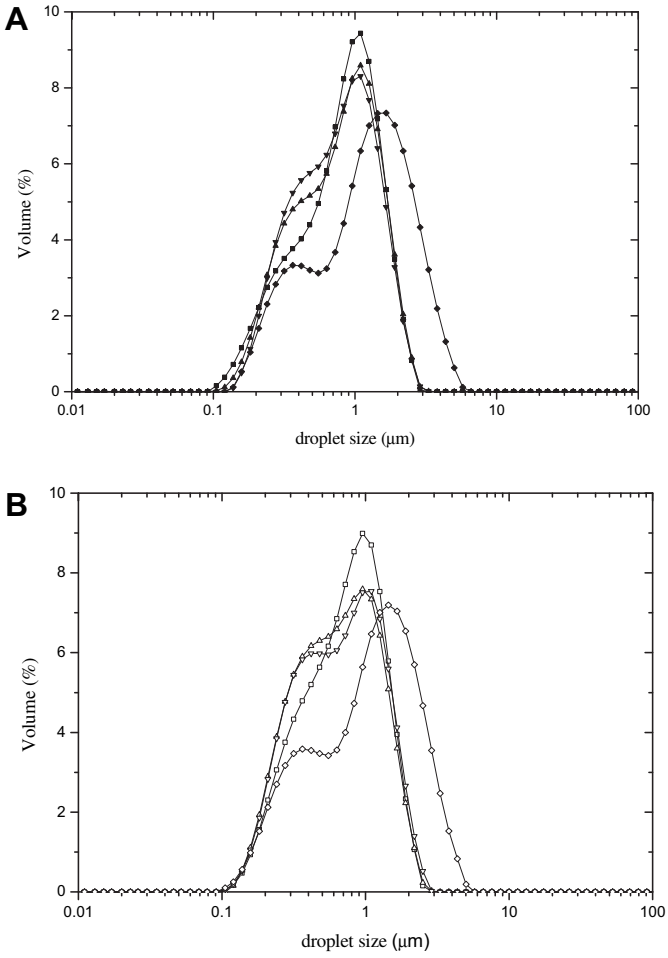

Fig. 3. Volume droplet size distribution (%) of 2% wt O/W HPMC emulsions homogenized with high intensity ultrasound at pH3 (A) and pH6 (B). E5LV (■,□), E15LV (▲,△), E50LV (▼,▽) and E4M (◆,◇).

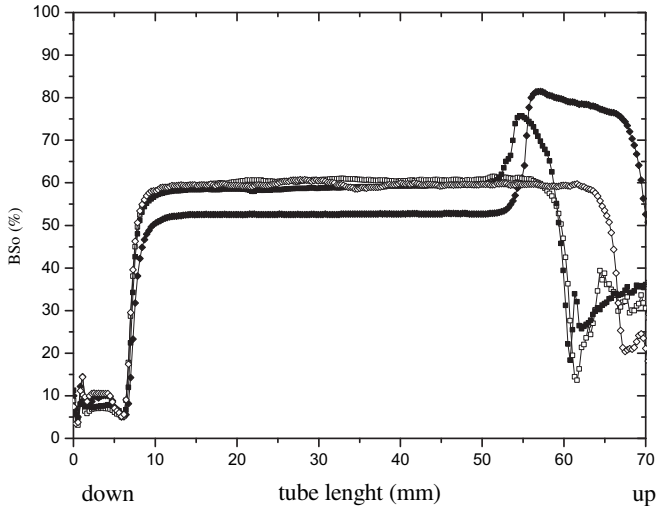

Fig. 4. Initial backscattering profiles (BSo%) of O/W HPMC emulsions prepared with Ultraturrax at pH3 (full symbols) and pH6 (empty symbols) for E5LV (■,□) and E4M (◆,◇).

emulsions homogenized with a high-pressure homogenizer, obtained smaller droplet sizes with the shorter chained and lower molecular weight HPMC.

Jafari, He, and Bhandari (2007) when studying O/W emulsions of D-limonene with maltodextrin and modified starch with mechanical agitation and ultrasound, found that D_{32} and D_{43} resulted three times higher for emulsions prepared by mechanical agitation. The droplet size distribution (volume %) was bimodal for this homogenizer.

Abismail, Canselier, Wilhelm, Delmas, and Gourdon (1999) studied comparatively emulsions of Tween 60 and sunflower oil prepared with mechanical agitation (UT) and ultrasound. For all the treatments times analyzed, they found that the D_{32} was higher for emulsions prepared with UT. The HIUS emulsions were less polidispersed and more stable during storage.

The differences are ascribed to the energy delivered to the system. When a mechanical agitator is used, the force involved is shear stress in laminar flow which does not produce a good rupture of the droplets. That is the reason for the presence of populations of higher sizes (droplets higher than 10 μm, Fig. 1). The cavitation is the cause for the droplets rupture during emulsification by high intensity ultrasound. There are also other phenomena like heat, dynamic agitation, shear rate and turbulence which cause physical and chemical changes in the system trough the generation and collapse of the cavities. The fast collapse of these cavities produce shear forces strong enough to rupture covalent bonds in polymeric materials (Guzey, 2002). Therefore, when emulsifying with HIUS, submicronic droplets are obtained (Jafari, He, & Bhesh, 2006).

The reduction of the droplet size is noticeable when emulsifying with HIUS (Tables 2 and 4). When comparing the HIUS emulsions, differences between them are found. Table 4 shows higher D_{32} and D_{43} for E4M emulsions at both pHs. Their volume distribution curves presented a bimodal distribution at higher sizes than that of the other three HPMCs at both pHs (Fig. 3). Loning, Horst, and Hoffmann (2002) sustained that the higher the viscosity of the continuous phase, the more difficult results the cavitation phenomenon induction. This could be the reason for the higher average diameters (Table 4) and a bimodal distribution (Fig. 3) for E4M emulsions.

As for UT emulsions, the flow parameters were obtained for USAI emulsions (Table 5). A higher value of consistent flow index

Table 4
Average diameters de Sauter (D_{32}), De Brouker (D_{43}), polidispersity and specific surface area (SSA) from 2% wt HPMCs emulsions prepared with HIUS.

HPMC	E4M		E50LV		E15LV		E5LV	
	pH3	pH6	pH3	pH6	pH3	pH6	pH3	pH6
D_{32} (μm)	0.81	0.71	0.62	0.55	0.62	0.59	0.61	0.54
D_{43}(μm)	1.53	1.37	0.92	0.84	0.94	0.87	0.96	0.81
polidispersity	2.05	2.09	1.71	1.85	1.69	1.81	1.59	1.59
SSA	7.37	8.47	9.68	11.00	1.59	10.20	9.77	11.20

Maximum standard deviation: 5%.

Table 5
Flow parameters of HPMC 2%wt emulsions prepared with HIUS, obtained by Ostwald model.

HPMC	pH3		pH6	
	K	*n*	*K*	*n*
E5LV	0.058 ± 0.005	0.916 ± 0.020	0.056 ± 0.004	0.968 ± 0.015
E15LV	0.129 ± 0.003	0.973 ± 0.005	0.121 ± 0.001	0.979 ± 0.003
E50LV	0.070 ± 1.165	0.820 ± 0.035	0.086 ± 0.018	1.170 ± 0.043
E4M	3.843 ± 1.694	0.749 ± 0.091	1.099 ± 0.028	0.978 ± 0.005

K: consistence flow index (N $m^{-2}s^{-n}$).
n: flow index.
$R^2 > 0{,}97$.

Table 6
Zeta potential for 2%wt HPMC emulsions prepared with UT and HIUS.

HPMC	E4M		E50LV		E15LV		E5LV	
pH	UT[a]	USAI[a]	UT[a]	USAI[a]	UT[a]	USAI[a]	UT[a]	USAI[a]
3	−1.040	−1.320	−0.683	−1.910	−1.080	−2.340	−1.510	−2.590
6	+0.239	+0.687	+0.125	+0.118	+0.253	+0.413	+0.291	+0.928

Maximum standard deviation: 1%.
[a] Average of at least $n = 5$.

(K) was exhibited by E4M emulsions at both pHs. The effect of the ultrasound is higher for emulsions stabilized with the higher molecular weight HPMCs. As we have discussed previously (Camino, Perez, & Pilosof, 2009) the ultrasound waves promotes a partial dehydration and/or modification in the E4M structure, provoking a global decrease in the emulsion viscosity.

Table 6 shows the superficial charge of HPMC droplets at pH3 and pH6 obtained by UT and HIUS. The same tendency observed for HPMC solutions (Camino et al., 2011) was observed for the emulsions, a negative charge at pH3 and a positive one at pH6. The absolute zeta potential value resulted significantly higher for HIUS emulsions, which is related with their lower droplet size (McClements, 1999).

3.2. HPMC emulsion stability during stationary storage at ambient temperature

3.2.1. Emulsion characterization immediately after homogenization

The term stability for an emulsion refers to the ability to resist changes in its properties through time. When higher the emulsion stability, lower the changes in its properties (McClements, 1999). The time during which the emulsion should be stable depends mainly from the nature of the food product (Dickinson, 1992). Some emulsions are generated during a stage of the manufacturing process, so they need to be stable only a few seconds, minutes or hours. Others emulsions must be stable during days, months or years before the consumption.

The emulsions with low volumetric relation between dispersed and continuous phases, like these HPMC emulsions, tend to destabilize by creaming. The flocculation presents a high influence in the creaming process and could favor the gravitational separation, depending on the droplets size and flocks structure (McClements, 1999; Palazolo, 2006).

After a period of stationary storage, a cream phase is observed in the top of the emulsion (concentration of droplets at the top). The low phase or serum is depleted in droplets.

In absence of external forces, the coalescence is a slow destabilization process, in comparison with creaming and flocculation. Therefore, with the exception of not effective homogenization process or emulsification agent, the coalescence takes place when the cream phase has been previously formed and the creaming and flocculation processes are in an advanced stage (Palazolo, 2006).

In a more concentrated dispersed phase, the droplets lose their mobility and could stay in an intimate contact during a long period which induces the coalescence (Palazolo, 2006). The nature of the colloidal interactions between the droplets and the interfacial film resistance would determine the destabilization degree (McClements, 1999). In consequence, the emulsion stability to coalescence was evaluated through the characteristics of the cream phase after the stationary storage (Palazolo, 2006).

The HPMCs emulsion stability was analyzed through the global backscattering profiles (BS%) as a function of tube length. These profiles constitute the macroscopic fingerprint of the emulsion sample at a given time (Alvarez Cerimedo et al., 2010; Mengual et al., 1999).

Although the main objective of this study is the evaluation of the global emulsion stability, the initial backscattering profiles give information of the microstructure of the recently prepared emulsions (BSo%) (Palazolo, 2006). Márquez, Palazolo, and Wagner (2005) have found a relation between BSo% and the D_{32} in soy stabilized emulsions.

Figs. 4 and 5 shows the initial backscattering profiles (BSo%) for HPMCs emulsions prepared with UT and HIUS, respectively. The BSo% depends not only on the droplet diameter but also on the

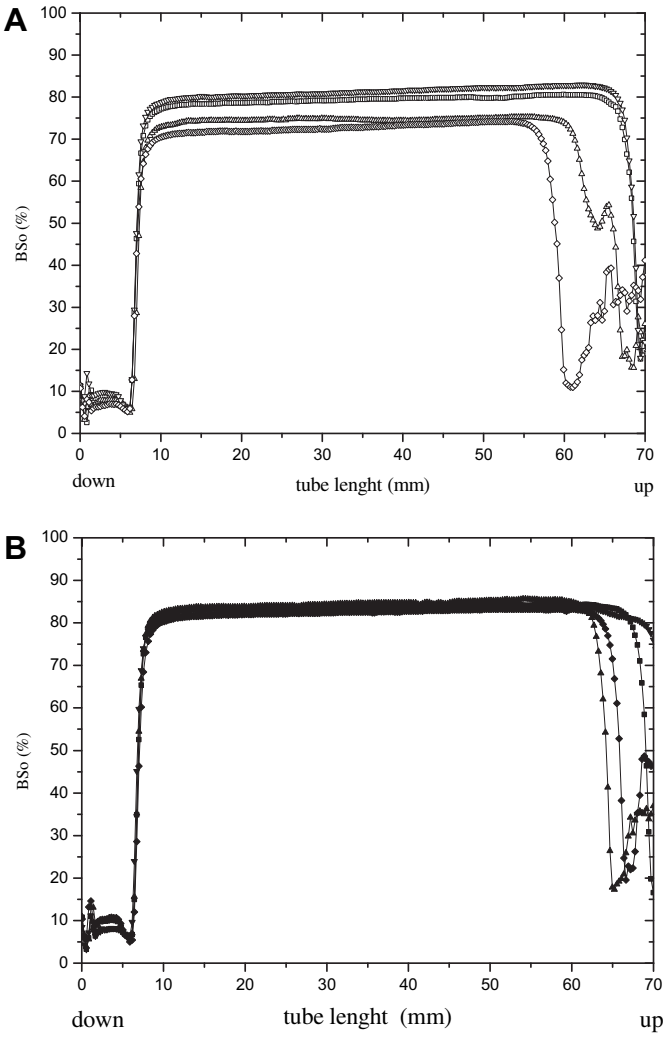

Fig. 5. Initial backscattering profiles (BSo%) of O/W HPMC emulsions prepared with high intensity ultrasound at pH3 (A) and pH6 (B) for E5LV (□,■), E15LV (△,▲), E50LV (▽,▼) y E4M (◇,◆).

volumetric fraction of the dispersed phase (φ) (Mengual et al., 1999; Palazolo, 2006). The BSo% profiles correspond to recently prepared emulsions, where the droplets are uniformly distributed in all the tube length, with a constant φ value. Then, the BSo% profiles depend only on the droplets diameter.

Fig. 4 shows the initial backscattering profiles for UT emulsions of two extreme viscosity HPMCs (Table 1, E4M and E5LV) at both pHs.

At constant volumetric fraction, the lower droplet size dispersed a higher quantity of light, which means higher percentage of BSo. This behavior could be appreciated in Fig. 4 where the E4M droplet size at pH3, dispersed a lower quantity of light and gave lower BSo% values. Then, the average diameters obtained for this emulsion resulted an order higher than for E5LV emulsions (Table 2).

There was a great increase in the BS at the top of the tube for pH3 emulsions, which suggested that immediately after homogenization, a migration occurred. For E4M emulsions the curve shape at the top of the tube indicated migration of individual droplets while for E5LV emulsions there was migration of aggregates/flocculates (Alvarez Cerimedo et al., 2010).

Higher BSo% were obtained for HIUS emulsions (Fig. 5) in comparison with UT emulsions (Fig. 4), indicating a lower droplet size (Table 4). There are higher differences between the HPMCs emulsions at pH3 while at pH6 these differences are almost absent (Fig. 5A and B).

Figs. 6 and 7 show the confocal images for HIUS recently prepared emulsions at pH3 and 6 respectively.

In optical microscopy, the easily observed droplets are those of higher size which dominate the creaming process. However, they are not the majority in number, then the optical images offer a partial information of the emulsion microstructure. It can be easily observed if the droplets are flocculated or not and the flocks characteristics (Palazolo, 2006).

Neither pH3 emulsions (Fig. 6) nor pH6 emulsions (Fig. 7) showed a higher tendency to flocculation. In all cases all the droplets are uniformly distributed, with low polidispersity in comparison with UT emulsions (Tables 2 and 4).

3.2.2. Creaming-flocculation stability

All the emulsions remained fully turbid along the tube during the 20 days of storage. Therefore, the transmission profiles were excluded from the analysis and only backscattering profiles were analyzed to evaluate the emulsions creaming kinetics.

Figs. 8 and 9 show the backscattering profiles, BS (%), for E4M and E5LV emulsions as examples, prepared with UT and USAI respectively.

A great variation with time could be observed in the BS (%) profiles for UT emulsions (Fig. 8), especially for E5LV emulsions, the HPMC with the lowest molecular weight and viscosity (Table 1). Even though E4M emulsions presented the higher droplet size (Table 2), the creaming and flocculation processes were minimized due to its higher viscosity as droplet velocity is lower.

The profiles of emulsions at pH3 greatly changed with storage time (Fig. 8A and B) in comparison to pH6 emulsions (Fig. 8C and D). The strong effect of pH on creaming would be the consequence of the pH effect on the viscoelasticity of HPMC films. In fact, the HPMCs films at pH3 have a very low viscoelasticity and poor solid

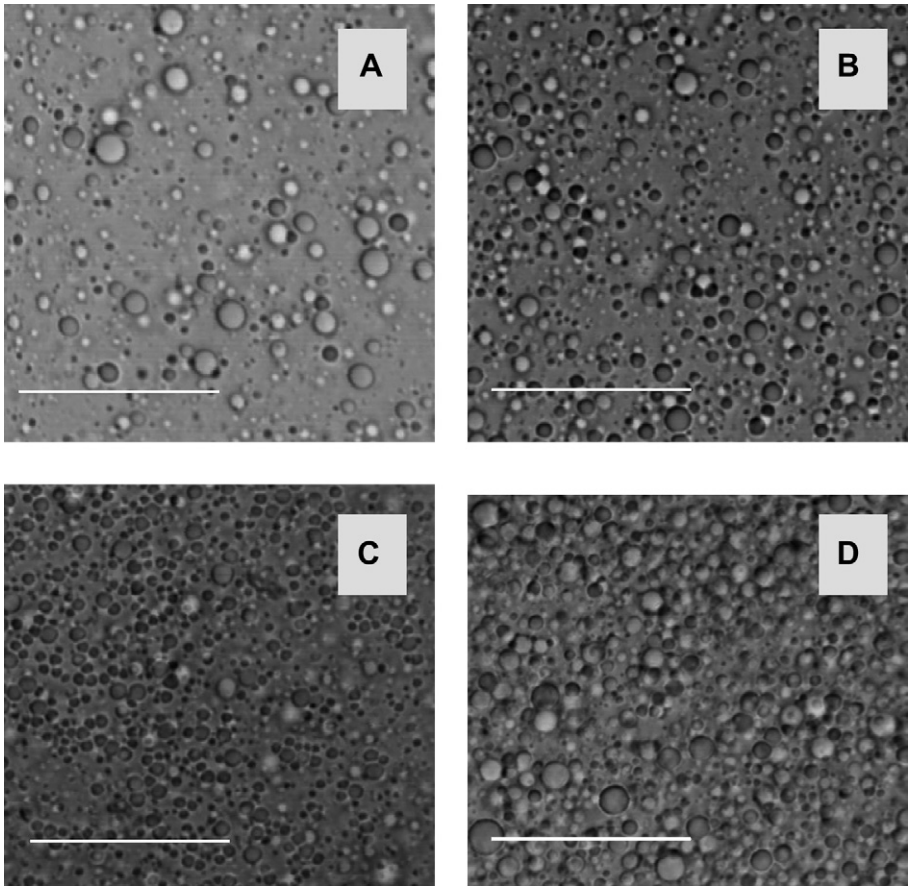

Fig. 6. Confocal images (60×, zoom 2.5×) of HPMC emulsions recently prepared with high intensity ultrasound at pH3. (A) E4M, (B) E50LV, (C) E15LV y (D) E5LV. White bars: 20 μm.

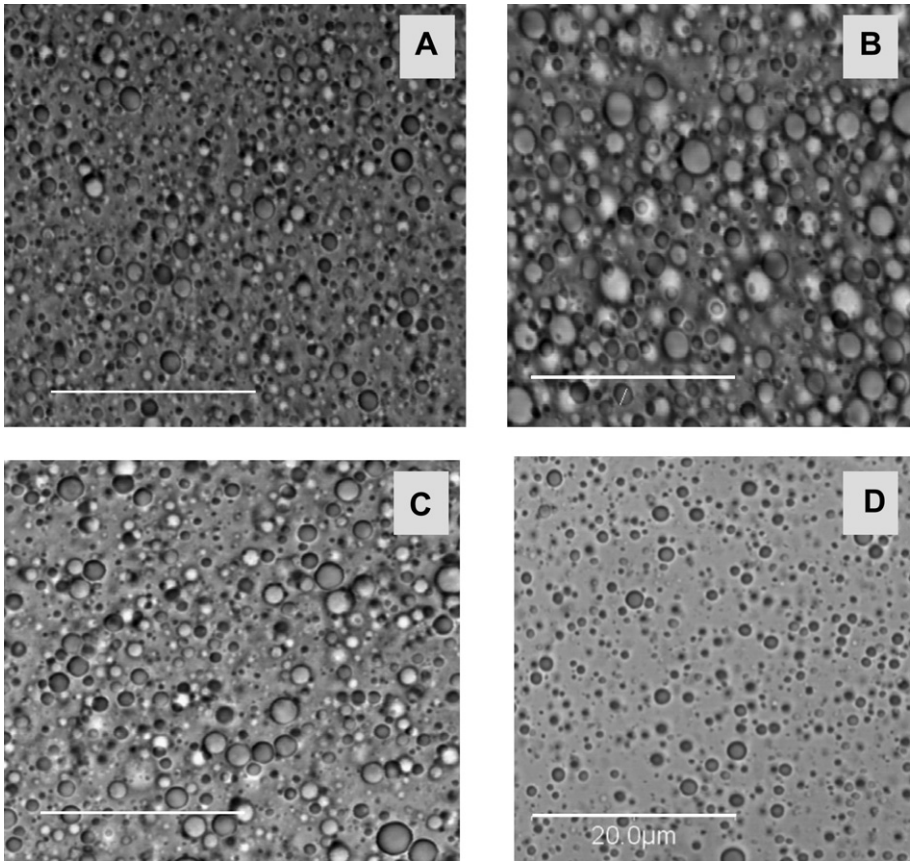

Fig. 7. Confocal images (60×, zoom 2.5×) of HPMC emulsions recently prepared by high intensity ultrasound at pH6. (A) E4M, (B) E50LV, (C) E15LV y (D) E5LV. White bars: 20 µm.

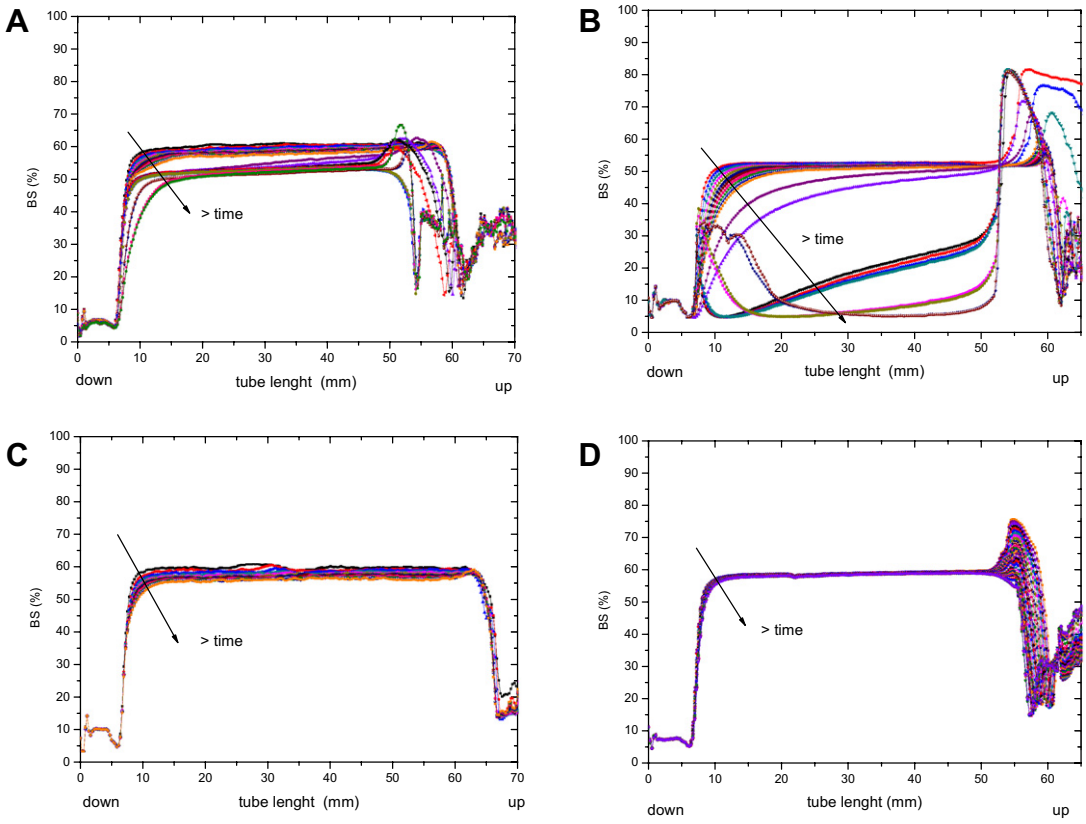

Fig. 8. Changes in backscattering profiles (BS%) as a function of sample height with storage time (samples were store for 20 days) of HPMC emulsions prepared by Ultraturrax at pH3 (A,B) and pH6 (C, D) for E4M (A,C) and E5LV (B,D). The arrows indicate the storage time. The creaming kinetics was analyzed in the 10–20 mm zone.

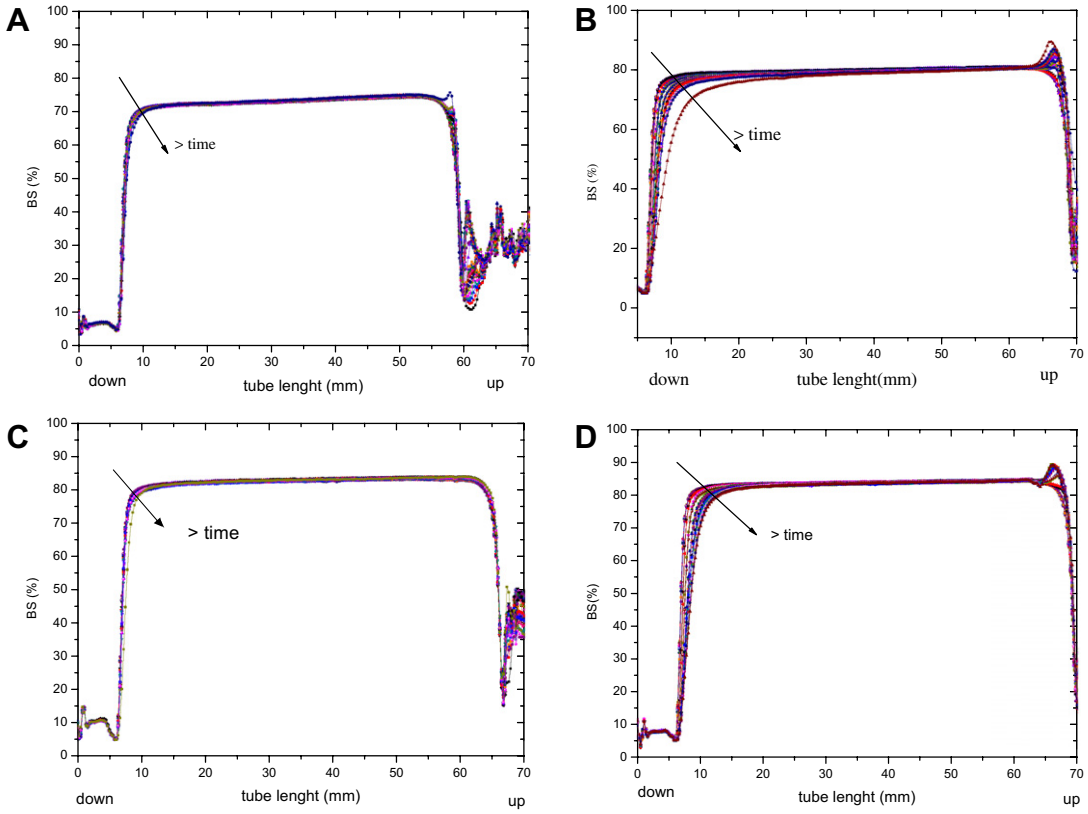

Fig. 9. Changes in backscattering profiles (BS%) as a function of sample height with storage time (samples were store for 20 days) of HPMC emulsions prepared by high intensity ultrasound at pH3 (A,B) and pH6 (C, D) for E4M (A,C) and E5LV (B,D). The arrows indicate the storage time. The creaming kinetics was analyzed in the 10–20 mm zone.

character (Camino et al., 2011) that enhances destabilization, specially in low viscosity emulsions.

For the emulsions at pH3 (Fig. 8A and B), and specially for E5LV (Fig. 8B) there was a great increase in the BS at the top of the tube, which suggested the migration of droplets. In addition, during that time, there was also a noticeable decrease in BS% profiles indicative of an increment in the mean particle size. This behavior may be associated to coalescence or flocculation (Alvarez Cerimedo et al., 2010).

The HIUS emulsions profiles (Fig. 9) showed less variation with storage time in accordance to their lower droplet diameter (Table 4), which is indicative of a higher stability. Only E5LV emulsions at both pHs, presented a small migration of individual particles (Fig. 9B and D), in accordance to its lower viscosity.

The slope of the plot of peak width vs. time is an indicator of the creaming rate; these kinetic constants (c) are given in Table 7 for UT and USAI emulsions at both pHs.

The higher the c value, the higher the degree of creaming (Palazolo, 2006). The creaming rate for both UT and HIUS emulsions resulted higher at pH3. This would be related to the higher droplet diameter obtained at this pH (Tables 2 and 4). For UT and HIUS emulsions the order for creaming rate resulted E5LV > E15LV > E50LV > E4M, reflecting the huge impact of the viscosity of the dispersed phase (Table 7) (Camino et al., 2011) and emulsion viscosity (Tables 3 and 5) in the creaming process. In these emulsions, E4M having the highest droplet diameters (Tables 2 and 4), presented the lowest creaming velocity because of the viscous effect.

Table 7
Slope of the linear zone evaluated from the peak-width vs. time curves (not presented) showing migration in the bottom part of emulsions.

HPMC	$C \times 10^2$ (mm/h)			
	UT		HIUS	
	pH3	pH6	pH3	pH6
E5LV	340.60 ± 0.13	291.90 ± 0.80	1.68 ± 0.15	1.05 ± 0.12
E15LV	154.25 ± 0.26	103.76 ± 1.02	1.43 ± 0.32	0.85 ± 0.11
E50LV	50.21 ± 1.11	43.04 ± 0.90	0.93 ± 0.20	0.57 ± 0.13
E4M	30.30 ± 1.51	27.20 ± 1.07	0.80 ± 0.11	0.44 ± 0.13

A great difference is observed between UT and HIUS emulsions, being the creaming constant (c) two orders lower for the last ones. This keeps relation with the lower droplet size of HIUS emulsions. The size distribution (Fig. 3) and the average diameters (Table 4) were similar for all the HPMCs, in addition to the low polidispersity. The populations were mainly monomodal with a predominant droplet size, also evident in the confocal images (Figs. 6 and 7).

The creaming rate would be higher than the flocculation rate in HIUS emulsions because of their low tendency to flocculate as detected by microscopy (Figs. 6 and 7) and also reflected in the BS% profiles shape (Fig. 9).

The UT emulsions presented a higher difference between D_{32} and D_{43} (Table 2), which is indicative of a higher tendency to destabilization (Gu et al., 2005). Also their higher polidispersity promoted (Table 2) the creaming and flocculation.

The same effect is observed when flocculation is analyzed. Fig. 10 shows the variation in the BS in the 20–50 mm zone of the tube for flocculation quantification for E4M and E5LV UT emulsions. The variation in the profiles is almost insignificant ($\Delta BS\% < 0.1\%$, Fig. 10) for all the emulsions indicating the absence of flocculation in the period analyzed. Nevertheless, E5LV

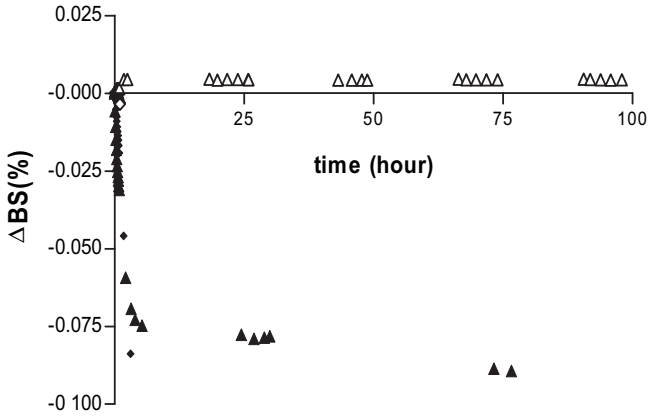

Fig. 10. Variation in the BS in the 20–50 mm zone for flocculation quantification for E4M and E5LV UT emulsions for E5LV (◆,◇) and E4M (▲,△) at pH3 and pH6 respectively.

emulsion at pH3 was the only one which presented a higher tendency to flocculation, in accordance with the results previously discussed.

3.2.3. Coalescence stability

The coalescence can be assessed by an increment in the D_{32} upon a period of storage (Carrera Sanchez & Rodriquez Patino, 2005), in this work 20 days. This is directly reflected in the droplets distributions curves. Cortez Muñoz, Chevalier Lucia, and Dumay (2009) when studying the storage under cooling of whey proteins-peanut oil emulsions prepared with a high-pressure valve, concluded that the similar distributions curves obtained for the emulsions before and after the chilled storage, indicated the absence of oil droplet coalescence.

Table 8 shows the D_{32} for UT and HIUS emulsions at both pHs upon storage time. The higher increment in the D_{32} for UT emulsions confirmed the occurrence of coalescence, mainly in E5LV emulsions (Table 8A).

It is evident that destabilization processes, creaming, flocculation and coalescence, are important in UT emulsions. The coalescence could be originated in the existence of a trimodal population (Fig. 1). The bigger droplet size grew due to the presence of the smaller ones and to the rupture of the interfacial film or because of the absence of polysaccharides in some zones of the surface droplets. The E4M emulsions presented a lower coalescence grade due to the higher viscosity that avoided the droplets getting closer.

Higher stability is achieved with HIUS emulsions. The D_{32} remained almost the same (Table 8B) during the time of storage. A little change was observed for E5LV emulsions, because of its lower viscosity.

Table 8
Average diameters, D_{32}, for E5LV and E4M emulsions prepared with UT (A) and HIUS (B) storage at ambient temperature for 20 days. Maximum standard deviation: 1%.

	pH3				pH6			
	Recently prepared	Day1	Day 5	Day 20	Recently prepared	Day1	Day 5	Day 20
(A)								
E4M	21.301	23.501	28.109	33.851	2.921	3.501	3.703	7.951
E5LV	1.441	2.532	10.931	28.137	1.811	2.602	5.327	9.304
(B)								
E4M	0.804	0.834	0.830	0.883	0.798	0.718	0.771	0.773
E5LV	0.614	0.624	0.756	0.772	0.537	0.587	0.699	0.769

4. Conclusion

A strong correlation between the properties of oil–water HPMC films (Camino et al., 2011), the viscosity of the continuous phase and the properties of the oil–water emulsions is highlighted in the present work, which is of great interest for a better control of these colloidal systems.

The homogenization method also had a strong influence in the emulsion characteristics. The higher energy delivered to the system by HIUS allowed the formation of emulsions of lower droplet diameters, more stable, if there is sufficient emulsifying agent in the continuous phase to cover the higher surface area created.

The pH effect was almost the same for both homogenization methods. At pH3 hydrophobic interactions between HPMC molecules are impeded so elastic films are not formed at the interface (Camino et al., 2011). Thus, there is coalescence during the formation of droplets upon emulsification, giving higher initial diameters than at pH6.

This in turn, leads the pH3 emulsions to destabilize quicker than pH6 emulsions, mainly when formed by UT, as a consequence of its higher initial D_{32}, polidispersity index, lower interfacial film elasticity and lower viscosity.

When comparing the performance of different HPMCs, the initial diameters kept correlation with the molecular weight (and viscosity) of the HPMC, being the lower molecular weight related with lower droplet diameters. This tendency is lower for emulsions formed by HIUS. E5LV (the lower HPMC molecular weight) generated the more elastic interfacial films due to its higher substitution in methyl groups (Camino et al., 2011). Nevertheless, E5LV presented higher creaming destabilization reflecting the importance of the viscosity of the continuous phase as a barrier for the droplet movement (McClements, 1999).

In conclusion, if it is important to obtain a lower average diameter, E5LV should be preferred among the HPMCs studied but a stabilizing agent should be added to increase the continuous phase viscosity and then slow down emulsion destabilization. If it is of interest a very stable emulsion, E4M should be used as emulsifying.

Acknowledgements

The authors acknowledge the support from Universidad de Buenos Aires, Agencia Nacional de Promoción Científica y Tecnológica and Consejo Nacional de Investigaciones Científicas y Técnicas de la República Argentina.

References

Abismail, B., Canselier, J., Wilhelm, A., Delmas, H., & Gourdon, C. (1999). Emulsification by ultrasound: droplet size distribution and stability. *Ultrasonics Sonochemistry, 6*, 75–83.

Alvarez Cerimedo, M. S., Huck Iriart, C., Candal, R., & Herrera, M. L. (2010). stability of emulsions formulated with high concentrations of sodium-caseinate and trehalose. *Food Research International*. doi:10.1016/j.foodres.2010.04.008.

Baeza, R., Carrera Sanchez, C., Pilosof, A. M. R., & Rodríguez Patino, J. M. (2004). Interactions of polysaccharides with [beta]-lactoglobulin spread monolayers at the air–water interface. *Food Hydrocolloids, 18*(6), 959–966.

Behrend, O., Ax, K., & Schubert, H. (2000). Influence of continuous phase on emulsification by ultrasound. *Ultrasonics Sonochemistry, 7*, 77–85.

Camino, N. A., Perez, O. E., Carrera Sanchez, C., Rodriguez Patino, J. M., & Pilosof, A. M. R. (2009). Hydroxypropylmethylcellulose surface activity at equilibrium and adsorption dynamics at the air–water and oil–water interfaces. *Food Hydrocolloids, 23*, 2359–2368.

Camino, N. A., Perez, O. E., & Pilosof, A. M. R. (2009). Modification of hydroxypropylmethylcellulose by high intensity ultrasound. *Food Hydrocolloids, 23*, 1089–1095.

Camino, N. A., Carrera Sanchez, C., Rodriguez Patino, J., & Pilosof, A. M. R. (2011). Hydroxypropylmethylcellulose at the oil–water interface. Part I. Bulk behaviour and dynamic adsorption as affected by pH. *Food Hydrocolloids, 25*, 1–11.

Carrera Sanchez, C., & Rodriguez Patino, J. M. (2005). Interfacial, foaming and emulsifying characteristics of sodium-caseinate as influenced by protein concentration in solution. *Food Hydrocolloids, 19*, 407–416.

Cornec, M., Wilde, P., Gunning, P., Mackie, A., Husband, F., Parker, M., et al. (1998). Emulsions stability as affected by competitive adsorption between an oil-soluble emulsifier and milk proteins at the interface. *Journal of Food Science, 63*, 39–43.

Cortez Muñoz, M., Chevalier Lucia, D., & Dumay, E. (2009). Characteristics of submicron emulsions prepared by ultra-high pressure homogenisation: effect of chilled or frozen storage. *Food Hydrocolloids, 23*, 640–654.

Courthaudon, J. L., & Dickinson, E. (1991). Competitive adsorption of lecithin and β-casein in oil in water emulsions. *Journal Agricultural of Food Chemistry, 39*, 1365–1368.

Daniels, R., & Barta, A. (1993). Preparation, characterization and stability assessment of oil-in-water emulsions with Hydroxypropylmethylcellulose as emulsifier. *Proceedings of Pharmaceutics Technology Conference, Elsinore*, pp. 51–60.

Daniels, R., & Barta, A. (1994). Pharmacopoeial cellulose ethers as oil in water emulsifiers 1. Interfacial properties. *European Journal of Pharmaceutical and Biopharmaceutical, 40*, 128–133.

Dickinson, E. (1992). *Introduction to food colloids*. Oxford: Oxford University Press.

Dickinson, E. (2001). Milk protein interfacial layers and the relationship to emulsion stability and rheology. *Colloids and Surfaces B: Biointerfaces, 20*, 197–210.

Dickinson, E. (2003). Hydrocolloids at interfaces and the influence on the properties of dispersed systems. *Food Hydrocolloids, 17*, 25–39.

Fernandez, P., André, V., Rieger, J., & Kühnle, A. (2004). Nano-emulsion formation by emulsion phase inversion. *Colloids and Surface A: Physicochemical Engeneering Aspects, 251*, 53–58.

Friberg, S. E., & Larsson, K. (1997). *Food emulsions* (3rd ed.). New York: Marcel Decker.

Galazka, V. B., Dickinson, E., & Ledward, D. A. (1996). Effect of high pressure on the emulsifying behaviour of b-lactoglobulina. *Food Hydrocolloids, 10*, 213–219.

Gu, Y., Decker, E., & McClements, D. J. (2005). Production and characterization of oil–water emulsions containing droplets stabilized by multilayer membranes consisting of β-lactoglobulin, ι-carrageenan and gelatin. *Langmuir, 21*, 5752–5760.

Guzey, D. (2002). Modification of protein structure and functionality using high-intensity ultrasound. Phd thesis, University of Tennessee.

Guzey, D., Kim, H. J., & McClements, D. J. (2004). Factors influencing the production of O/W emulsions stabilized by b-lactoglobulin–pectin membranes. *Food Hydrocolloids, 18*, 967–975.

Hayakawa, K., Kawaguchi, M., & Kato, T. (1997). Protective colloidal effects of hydroxypropyl methylcellulose on the stability of silicone oil emulsions. *Langmuir, 13*, 6069–6073.

Huang, X., Kakuda, Y., & Cui, W. (2001). Hydrocolloids in emulsions: particle size distribution and interfacial activity. *Food Hydrocolloids, 15*, 533–542.

Jafari, S., He, Y., & Bhesh, B. (2006). Nano-emulsification production by sonication and microfluidization – a comparison. *International Journal of Food Properties, 9*, 475–485.

Jafari, S., He, Y., & Bhandari, B. (2007). Production of sub-micron emulsions by ultrasound and microfluidization techniques. *Journal of Food Engineering, 82*, 478–488.

Kiekens, F., Vermeire, A., Samyn, N., Demeester, J., & Remon, J. P. (1997). Optimization of electrical conductance measurements for the quantification and prediction of phase separation in o/w emulsions, containing hydroxypropylmethylcellulose as emulsifying agents. *International Journal of Pharmaceutics, 146*, 239–245.

Leroux, J., Langendorff, V., Schick, G., Vaishnav, V., & Mazoyer, J. (2003). Emulsion stabilizing properties of pectin. *Food Hydrocolloids, 17*, 455–462.

Loning, J., Horst, C., & Hoffmann, U. (2002). Investigation on the energy conversion in sonochemical processes. *Ultrasonics Sonochemistry, 9*, 169–179.

Márquez, A. L., Palazolo, G. G., & Wagner, J. R. (2005). Emulsiones tipo crema preparadas a base de leche de soja I: Estudios de estabilidad y determinación de las formulaciones. Grasas y Aceites. *International Journal of Fats and Oils, 56*, 59–66.

McClements, D. J. (1999). *Food emulsions. Principles, practice and techniques*. New York: CRC Press.

McClements, D. J. (2004). Protein-stabilized emulsions. *Current Opinion in Colloid and Interface Science, 9*, 305–313.

Mengual, O., Meunier, G., Cayré, I., Puech, K., & Snabre, P. (1999). Turbiscan MA 2000: multiple light scattering measurement for concentrated emulsion and suspension instability analysis. *Talanta, 50*, 445–456.

Mitidieri, F., & Wagner, J. (2002). Coalescence of O/W emulsiones stabilized by whey and isolate soybean proteins. Influence of thermal denaturation, salt adittion and competitive interfacial adsorption. *Food Research International, 35*, 547–557.

Palazolo, G. (2006). Formación y estabilidad de emulsiones O/W preparadas con proteínas nativas y desnaturalizadas de soja. PhD thesis, Universidad Nacional de La Plata.

Perez, O. E., Carrera Sanchez, C., Rodriguez Patino, J. M., & Pilosof, A. M. R. (2006). Thermodynamics and dynamics characteristics of hydroxypropylmethylcellulose adsorbed films at the air water interface. *Biomacromolecules, 7*, 388–393.

Perez, O. E., Wargon, V., & Pilosof, A. M. R. (2006). Gelation and structural characteristics of incompatible whey proteins/hydroxypropylmethylcellulose mixtures. *Food Hydrocolloids, 20*, 966–974.

Porras, M., Solans, C., Gonzalez, C., Martinez, A., Guinart, A., & Gutierrez, J. M. (2004). Studies of formation of W/O nano-emulsions. *Colloids and Surface A: Physicochemical Engeneering Aspects, 249*, 115–118.

Relkin, P., & Sourdet, S. (2005). Factors affecting fat droplet aggregation in whipped frozen protein-stabilized emulsions. *Food Hydrocolloids, 19*, 503–511.

Schulz, M., & Danields, R. (2000). Hydroxypropylmethylcellulose (HPMC) as emulsifier for submicron emulsions: influence of molecular weight and substitution type on the droplet size after high-pressure homogenization. *European Journal of Pharmaceutics and Biopharmaceutics, 49*, 231–236.

Sjöblom, J. (1996). *Emulsions and emulsions stability*. In *Surfactant science series, Vol. 61*. New York: Marcel Decker.

Solans, C., Izquierdo, P., Nolla, J., Azemar, N., & Garcia-Celma, M. (2005). Nano-emulsions. *Current Opinion in Colloid and Interface Science, 10*, 102–110.

Sun, W., Sun, D., Wei, Y., Liu, S., & Zhang, S. (2007). Oil-in-water emulsions stabilized by hydrophobically modified hydroxyethyl cellulose: adsorption and thickening effect. *Journal of Colloid and Interface Science, 311*(1), 228–236.

Ventureira, J., Martinez, E., & Añon, M. (2010). Stability of oil:water emulsions of amaranth proteins. Effect of hydrolysis and pH. *Food Hydrocolloids, 24*, 551–559.

Walstra, P. (1993). Principles of emulsion formation. *Chemical Engineering Science, 48*, 333.

Weiss, J., Takhistov, P., & McClements, J. (2006). Funtional materials in food nanotechnology. *Journal of Food Science, 71*, 107–116.

Wollenweber, C., Makievski, A. V., Miller, R., & Daniels, R. (2000). Adsorption of hydroxypropyl methylcellulose at the liquid/liquid interface and the effect on emulsion stability. *Colloids and Surfaces A: Physicochemical and Engineering Aspects, 172*(1–3), 91–101.

Yuguchi, Y., Urakawa, H., Kitamura, S., Ohno, S., & Kajiwara, K. (1995). Gelation mechanism of methylhydroxypropylcellulose in aqueous solution. *Food Hydrocolloids, 9*, 173–179.